

Supporting Information

Constructing a Novel Hierarchical Structured NH₄-Co-Ni Phosphate toward Ultrastable Aqueous Hybrid Capacitor

Zhaoyang Chen¹, Ding-Bang Xiong², Xuejiao Zhang¹, Hongnan Ma¹, Meirong Xia¹,
Yufeng Zhao^{1*}

¹*Key Laboratory of Applied Chemistry, Yanshan University, Qinhuangdao, 066004, China.
Corresponding Email: *yufengzhao@ysu.edu.cn*

²*State Key Laboratory of Metal Matrix Composites, Shanghai Jiao Tong University, Shanghai
200240, China*

Experimental Section

Preparation of cobalt and nickel hydroxide precursor

With a simple production method, 0.25 g $\text{Ni}(\text{NO}_3)_2 \cdot 6\text{H}_2\text{O}$ (0.865 mmol) and 0.25 g $\text{Co}(\text{NO}_3)_2 \cdot 6\text{H}_2\text{O}$ (0.865 mmol) were dissolved in 60 mL of deionized water, magnetic stirred for fifteen minutes to obtain a light pink solution, and then 3.8 ml ammonia solution (2 mol/L) was dropwise added. After stirring for 30 mins, the solution was transferred into an 80 mL Teflon-lined stainless-steel autoclave and heated at 120 °C for 4 h. After cooling to room temperature naturally, the grey precipitate was collected and successively washed with deionized water and ethanol for several times, Respectively. The product then dried in vacuum oven at 80 °C for 10 h.

Preparation of hierarchical porous carbon (HPC)

HPC was prepared as reported previously.²³ Artemia cyst shells were cleaned with deionized water, dried at 80°C for 72 h, then ball-milled for 6 h at a speed of 300 rpm. The carbonization of ball-milled Artemia cyst shells was carried out in a tube furnace according to the following steps: (1) the Artemia cyst shells were heated to 300°C at Ar gas atmosphere with a heating rate of 5°C min⁻¹ and maintain for 3 h for pre-carbonization, then heated up to 700°C at 5°C min⁻¹ and keep for 4 h. (2) The obtained products were sonicated in 67 wt% HNO_3 for 80 mins, then washed with deionized water and dried at 80°C for 12 h. (3) The resulting product was mixed with potassium hydroxide with a weight ratio of 1:2, then heated to 700°C at 10°C min⁻¹ in Ar atmosphere and held for 1 h, the final product was named as HPC.

Supporting Figures

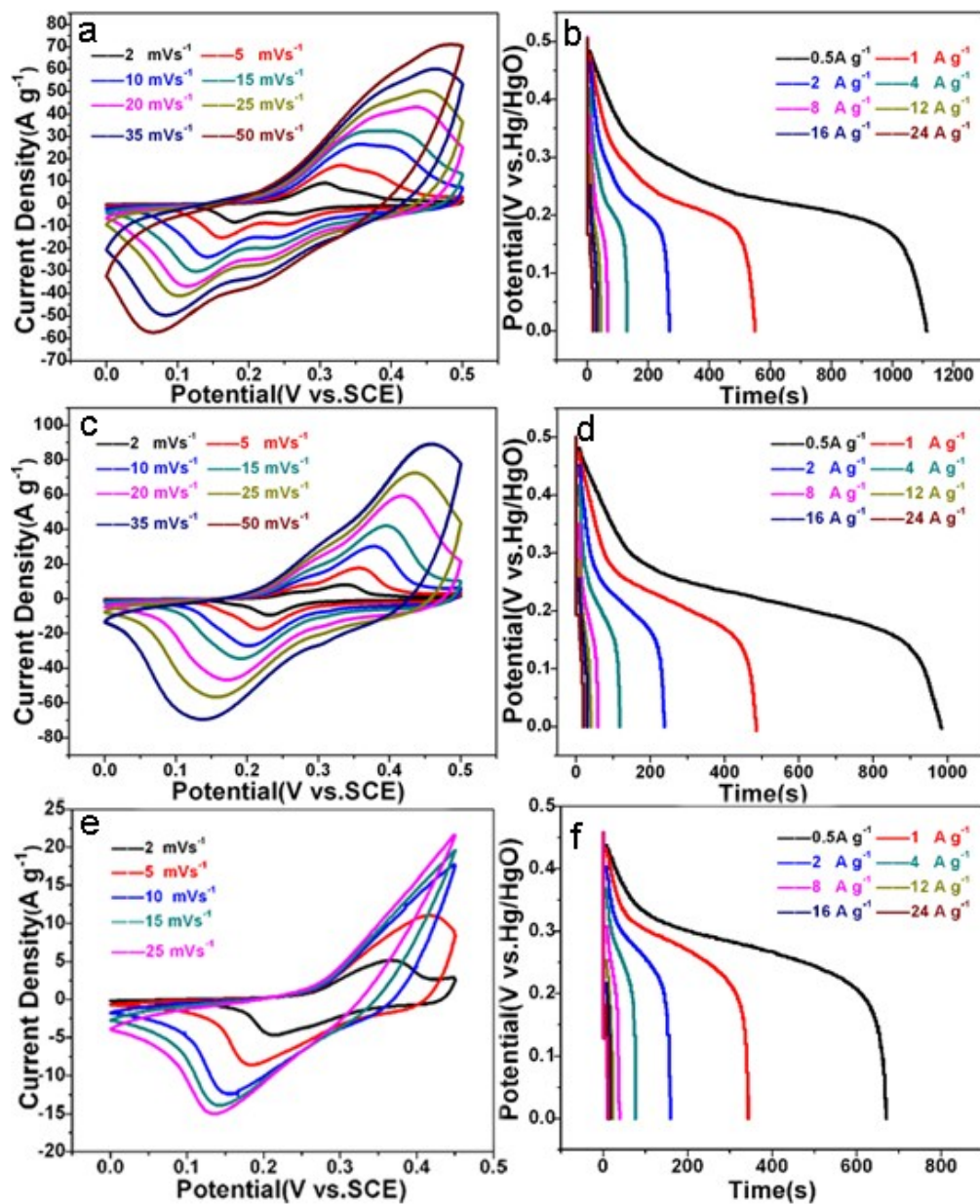


Figure S1. CV curves at different scan rates at different reaction stage (a) 1h, (c) 4h, (e) 24h, GCD curves (b) 1h, (d) 4h, (f) 24h.

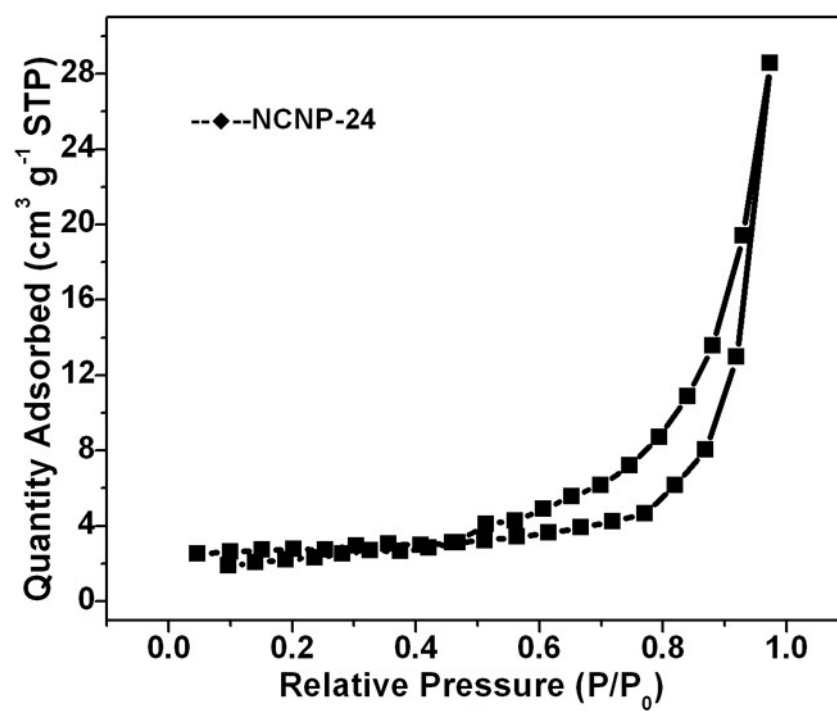


Figure S2. N_2 adsorption-desorption isotherms at 77 K of the NCNP-24 sample.

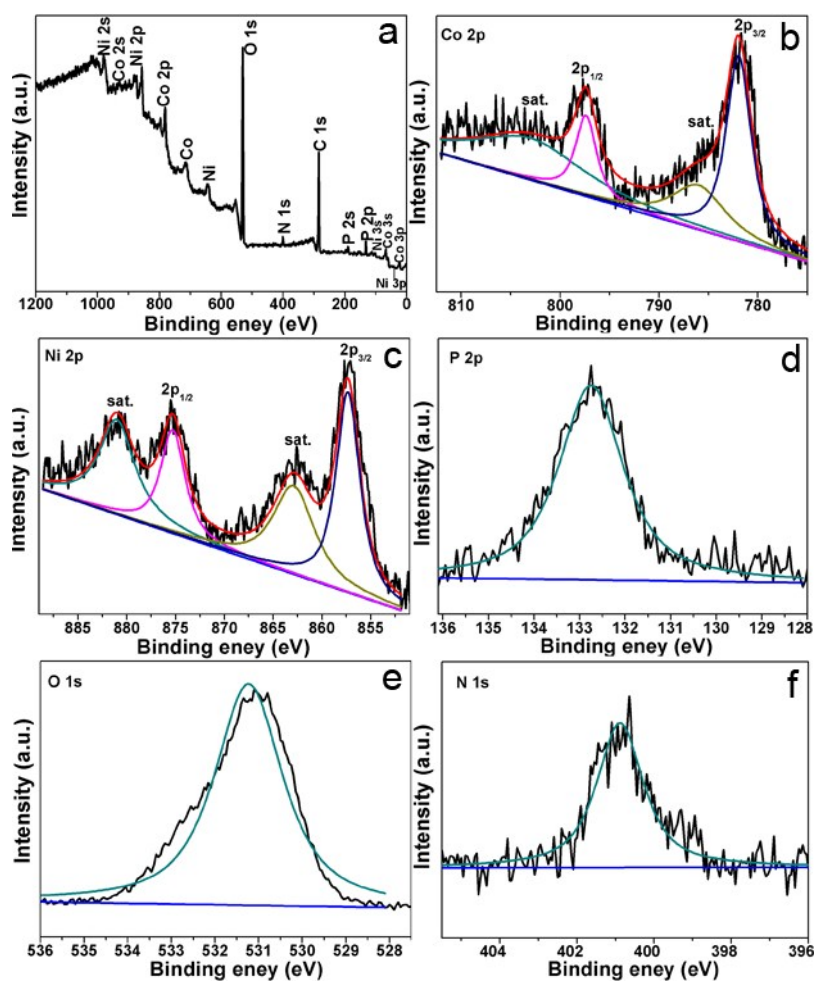


Figure S3. XPS spectra of the NCNP-2: (a) survey spectrum, (b) Co 2p, (c) Ni 2p, (d) P 2p, (e) O 1s, and (f) N 1s.

The X-ray photoelectron spectroscopic (XPS) spectra of the NCNP-2 were measured by a Thermo Scientific ESCALAB 250Xi photoelectron spectrometer using Mg-K α as the exciting source (1253.6 eV). Fig. S3a shows the survey spectrum of NCNP-2, which can be assigned as the characteristics of Co, Ni, P, O, N, and C respectively. No other element is found from the XPS spectrum, demonstrating the high purity of the sample. The high-resolution Co 2p and Ni 2p spectra were fitted by the Gaussian fitting method, and both of them are well fitted with two spin-orbit doublets and two

shake-up satellites (marked 'Sat.'). For the Co 2p XPS spectrum, the first doublet is situated at 780.9 and 796.5 eV, the second is located at 781.9 and 798.1 eV, corresponding to a spin-orbit splitting value of Co 2p_{3/2} and Co2p_{1/2} of 15.6 eV and 16.2 eV, can be ascribed to Co³⁺ and Co²⁺, respectively (Fig. S3b). For the Ni 2p XPS spectrum, the binding energy at 856.1 eV in Ni 2p_{3/2} and 873.3 eV in Ni 2p_{1/2}, and the binding energy at 857.6 eV in Ni 2p_{3/2} and 875.4 eV in Ni 2p_{1/2}, which are characteristic of Ni²⁺ and Ni³⁺, respectively (Fig. S3c)^{1,2}. The high resolution XPS spectra of P 2p, O 1s and N 1s are shown in Fig. S3d-3f, corresponding to binding energy peaks at 132.8, 531.2, and 400.9 eV, respectively.

Reference

1. H. C. Chen, J. J. Jiang, Y. D. Zhao, L. Zhang, D. Q. Guo and D. D. Xia, *J. Mater. Chem. A*, 2015, **3**, 428-437.
2. J. C. Zhang, Y. Yang, Z. C. Zhang, X .B. Xu and X. Wang, *J. Mater. Chem. A*, 2014, **2**, 20182-20188.

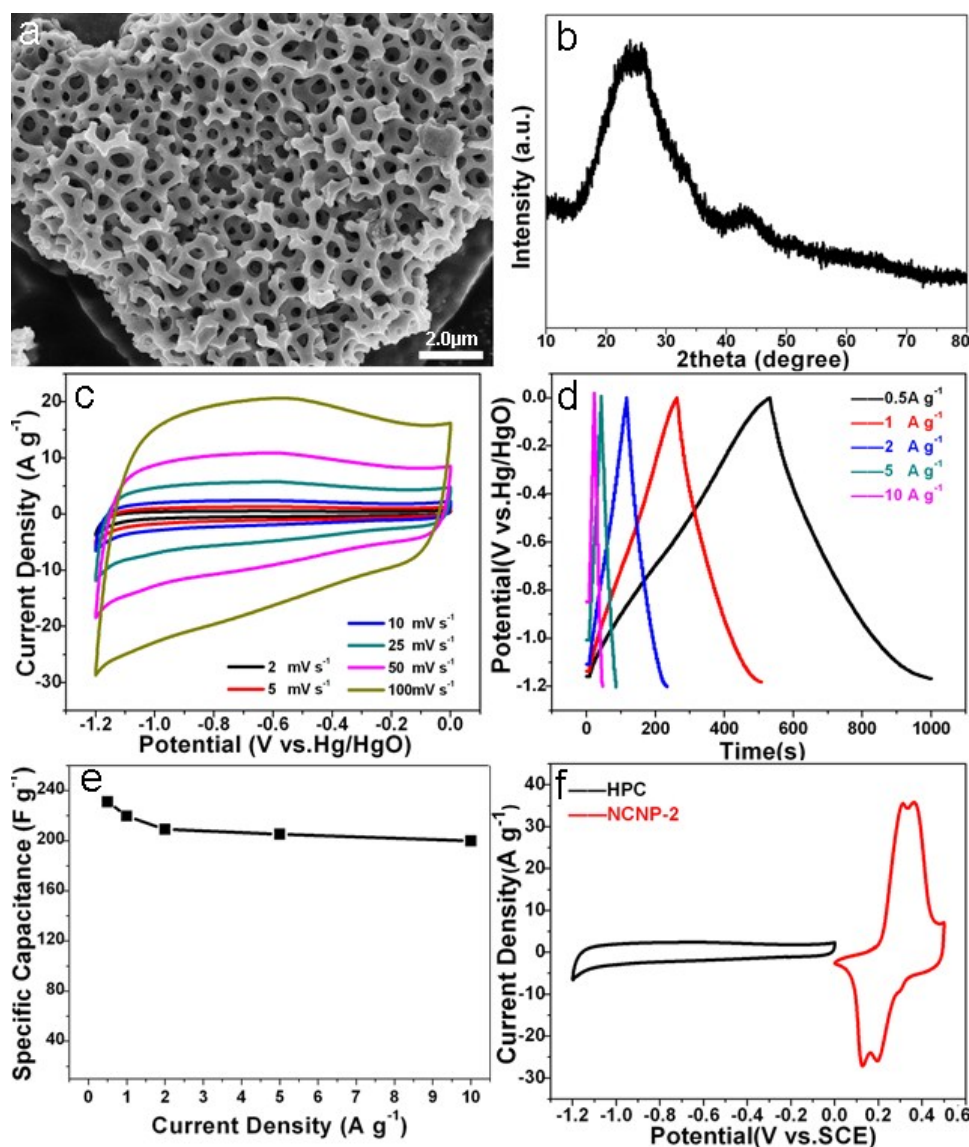


Figure S4. FESEM image (a), XRD pattern (b), CV curves at different scan rates (c), GCD curves at different current densities (d), SC as a function of discharge current densities (e) of HPC, and CV curves of NCNP-2 and HPC at 10 mV s⁻¹ (f).

Fig. S4a shows the FESEM image of the HPC derived from Artemia cyst shells (AS), the hierarchical porous structure of the AS is well preserved. **Fig. S4b** shows the XRD patterns of the as prepared HPC. Broad bumps at a 2θ of about 26.1° and 43° corresponding to the (002) and (100) reflections of a graphitic-type lattice are observed, indicating the mainly amorphous characteristics of the HPC. **Fig. S4c**

shows CV curves of HPC electrodes tested with a three electrode system in the potential range of -1.2~0 V with scan rates from 2 to 100 mV s⁻¹ in 6M KOH. **Fig. S4d** shows GCD curves of HPC at different current densities from 0.5~10 A g⁻¹. The corresponding SC as a function of discharge current densities is calculated as shown in **Fig. S4e**, the HPC delivered a SC of 230 F g⁻¹ at 0.5 A g⁻¹ which remains 199.8 F g⁻¹ at 10 A g⁻¹. **Fig. S4f** shows the CV curves of HPC and the as prepared NH₄CoNiP at the scan rate of 10 mV s⁻¹, the different operation voltages of the NH₄CoNiP electrode (0~0.5 V) and HPC electrode (\approx -1.2~0 V) indicate a perfect match on the potential windows for a hybrid capacitor.

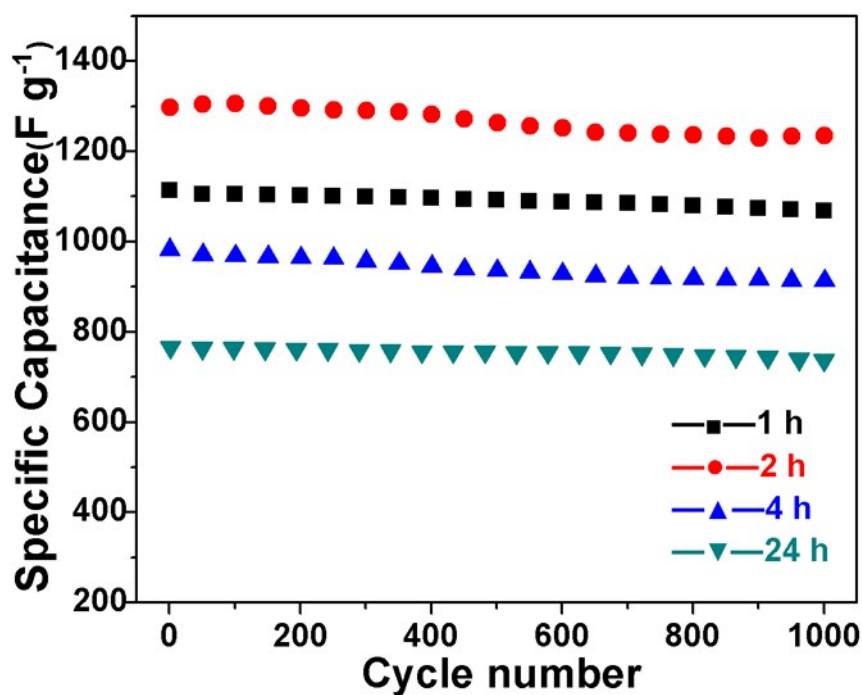


Figure S5. Cycling performance of the products in a three-electrode electrochemical cell at a constant current density of 4 A g^{-1} .

The cycling stability of NCNP-1, NCNP-2, NCNP-4 and NCNP-24 were also tested in a three-electrode system within a potential window of 0 to 0.5 V, and a capacity retention of 95.8 %, 95.7 %, 93 % and 97.2 % after 1000 charge/discharge cycles was obtained for the four products respectively.

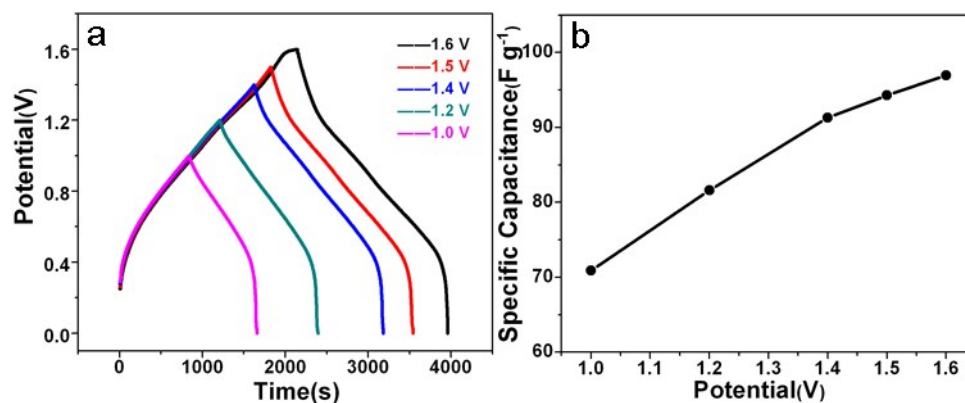


Figure S6. Electrochemical performance of the NCNP//HPC hybrid capacitor: (a) galvanic charge/discharge plots at different potentials, (b) specific capacitances as a function of discharge current densities.

The electrochemical performance of the as fabricated HC was measured with different voltage window (Fig. S6). As can be seen, with the increase of the potential window (from 1V to 1.6V), the specific capacitance of HC increases significantly, indicating the more efficient utilization of the positive electrode material at a larger voltage range.